Thin Solid Films 519 (2011) 7276–7279

Contents lists available at ScienceDirect

Thin Solid Films

journal homepage: www.elsevier.com/locate/tsf

Near-interface doping by ion implantation in $Cu(In,Ga)Se_2$ solar cells

J. Haarstrich [a,*], H. Metzner [a], C. Ronning [a], T. Rissom [b], C.A. Kaufmann [b], H.W. Schock [b], W. Mannstadt [c], E. Rudigier-Voigt [c], V. Scheumann [c]

[a] Institut für Festkörperphysik, Friedrich Schiller Universität Jena, Max-Wien-Platz 1, 07743 Jena, Germany
[b] Helmholtz Zentrum Berlin für Materialien und Energie, Solar Energy Research, Institute for Technology, Lise-Meitner-Campus, Hahn-Meitner-Platz 1, 14109 Berlin, Germany
[c] Schott AG, Hattenbergstraße 10, 55122 Mainz, Germany

ARTICLE INFO

Available online 21 December 2010

Keywords:
$Cu(In,Ga)Se_2$
Thin-film solar cells
Ion implantation
EQE
Surface inversion
Cd diffusion
Annealing

ABSTRACT

$Cu(In,Ga)Se_2$ absorber layers were implanted with 20 keV Cd ions in order to investigate the influence of changes in the near-interface doping profile. Modifications in this region are shown by AMPS-1D simulations to have substantial impact on solar cell properties. Ion implantation and subsequent thermal annealing steps were monitored by SIMS measurements to control the thermal diffusion of the dopant. Solar cells both with and without CdS buffer layer were made from the implanted absorbers and characterized by j-V and EQE measurements. These experimental results in conjunction with simulations of the quantum efficiency show that a well-defined type-inversion of the implanted layer can be achieved by low-energy ion implantation.

1. Introduction

High-efficiency solar cells based on $Cu(In,Ga)Se_2$ (CIGS) absorber layers commonly use CdS as an n-type buffer layer, but other materials such as In_xS_y [1] or Zn(S,O,OH) [2] have also been applied successfully. The basic function of the buffer layer is to form the p–n heterojunction as such that a low interface recombination is obtained. A reduction of recombination can be reached either by a decrease in interface defect density or by driving the Fermi-level close to the conduction band at the interface [3]. This so called n-type surface inversion implies a lower concentration of holes at the interface and therefore leads to a reduction of possible recombination partners for electrons. This way, low recombination rates are possible despite the presence of a considerable concentration of interface defects. At the well designed CIGS/CdS interface, a stable surface inversion is most probably formed during CdS deposition in the chemical bath, whereas it is discussed whether this is due to Cd diffusion [4,5] into the surface and/or the reestablishment of a natural n-type surface of CIGS through the surface treatment in the bath [6]. However, a stable n-type surface layer should decouple junction functionality from interface quality which would allow to completely omit the buffer layer.

To directly study the influence of an inversion of the surface layer, ion implantation shall be used to introduce well-defined doping profiles in the near-interface region of the absorber. In this contribution, this approach is proposed and described in detail, and the influence of the implantation on solar cell properties is analyzed.

2. Simulations

For further illustration of these principles, numerical simulations are performed with the software AMPS-1D [7]. All simulation results were also confirmed with SCAPS-1D 2.8 [8]. As a reference case for a high efficiency solar cell, base line parameters are adopted from the dissertation work of Markus Glöckler (base case) [9]. It contains a three-layer structure of ZnO/CdS/CIGS (Fig. 1(A)) and yields very good solar cell characteristics with an efficiency above 18% (Fig. 2(A)). If the CdS layer is simply removed from the stack (Fig. 1(B)) the high diode quality is preserved in the simulation (Fig. 2(B)), but a strong decrease in open-circuit voltage can be observed experimentally. This discrepancy can be solved if interface recombination is taken into account which is presumed to be significant in this case, whereas it was shown to be negligible in the reference case [9]. This is done by introducing an interface layer (Fig. 1(C)) with a concentration of mid-gap defects of 2.5×10^{12} cm^{-2} which was adjusted to model the j–V characteristics of a real buffer-less solar cell (Fig. 2(C)). If we now introduce an n-type surface layer in the CIGS absorber (Fig. 1(D), $N_D = 10^{18}$ cm^{-3}, d = 25 nm corresponding to the experiment), we are able to move the p–n junction away from the interface (buried junction) and an n-type surface is reestablished. Therefore, high-quality diode behavior can be recovered including open-circuit voltages above 600 mV and a fill factor above 75% (Fig. 2(D)). This is possible despite a high concentration of interface defects and thus should be independent of the buffer configuration. Hence, if the inversion of the surface layer is successful, the solar cell properties should be more or less the same with and without CdS buffer layer. The losses in short-circuit current density are due to absorption losses in the n-type layer (as shown in Section 4) and can be minimized for reduced n-type layer thickness.

* Corresponding author. Tel.: +49 3641 947313; fax: +49 3641 947302.
E-mail address: jakob.haarstrich@uni-jena.de (J. Haarstrich).

0040-6090/$ – see front matter
doi:10.1016/j.tsf.2010.12.090

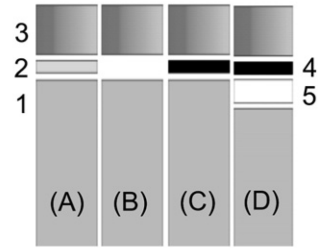

Fig. 1. Illustration of the layer structures used in AMPS-1D simulations. Simulation cases: (A) reference, (B) without CdS, (C) without CdS, with interface recombination, (D) without CdS, with interface recombination, with n-type surface layer. Layers: 1 CIGS, 2 CdS, 3 ZnO, 4 Interface layer, 5 n-type surface layer.

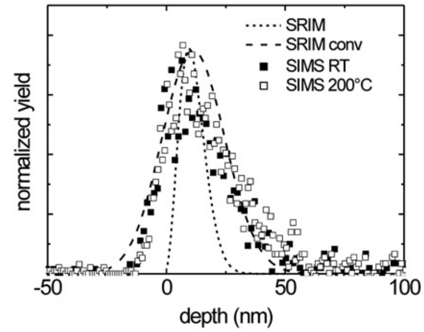

Fig. 3. Depth profiles of ^{114}Cd implanted in $Cu(In_{0.7}Ga_{0.3})Se_2$ with a fluence of 1.4×10^{15} cm^{-2} and an energy of 20 keV as measured with SIMS before and after annealing at 200 °C in inert gas. In addition, SRIM profiles are plotted before and after convolution with the SIMS resolution (Gaussian function, w = 12 nm, determined from onset of the CIGS-layer elements).

3. Experimental details

CIGS absorber layers were deposited on Mo-coated soda-lime glass by multi-stage co-evaporation at the Helmholtz Zentrum Berlin as described elsewhere [10]. The composition was analyzed by means of X-ray fluorescence (XRF) and yielded slightly Cu-poor stoichiometry (Cu/III = 0.9) and a Ga-content of approximately Ga/(Ga + In) = 0.3. Subsequently, ion implantation was performed at the accelerator facilities at the university in Jena using ^{114}Cd ions with an energy of 20 keV. Cd was chosen as a possible n-type dopant in $Cu(In,Ga)Se_2$. All results shown here correspond to an ion fluence of 4.2×10^{15} cm^{-2}. In Fig. 3, the depth profile is shown which was generated with the Monte-Carlo-Code SRIM [11]. The simulation was performed at normal incidence and using parameters for atomic binding energies suggested by SRIM (displacement energy 25 eV, lattice binding energy 3 eV, surface binding energy 3.52, 2.49, 2.14 and 2.82 eV for Cu, In, Ga and Se, respectively). It yields a maximum concentration of 7 at.% of Cd in a depth of about 10 nm, a decrease by a factor of ten at 25 nm and a concentration below the intrinsic doping level of around 10^{16} cm^{-3} at 50 nm. Using the simulation data given above, a sputter yield of around 7 nm is calculated by SRIM which would lead to a reduced implantation depth of 7 nm and a relative loss of Cd of around 8%. The sputtering effect may also have an influence on the surface stoichiometry. Finally, solar cells were fabricated from these implanted absorbers by depositing the front contact both with and without CdS buffer and an iZnO–ZnO:Al double layer.

Ion implantation is accompanied by defect creation, in this case in the order of 1000 defects per ion (vacancies calculated with SRIM). Therefore, annealing is needed which was performed by a heat-treatment of the finished device in air at 200 °C for 30 min. This procedure is known to preserve solar cell properties of standard CIGS cells [6,12], whereas the use of higher temperatures is found to lead to degradation (not shown, see also [12,13]). Before and after the annealing step, Cd depth profiles were measured on the implanted absorbers using secondary ion mass spectroscopy (SIMS) in order to check for diffusion of the implanted Cd ions. SIMS was measured at Schott AG Mainz. For those samples, annealing was performed in inert gas atmosphere in order to rule out the influence of oxygenation on SIMS analysis. As can be seen from Fig. 3, no change in the Cd depth distribution can be detected after annealing at 200 °C. Therefore, significant diffusion of the implanted Cd ions can be excluded at this temperature.

Furthermore, current density–voltage (j–V) characteristics of the solar cells were measured under standard AM1.5 illumination conditions. External quantum efficiency (EQE) measurements were performed at zero bias-voltage and under 11% AM1.5-equivalent white bias-light condition.

4. Results and discussion

In Fig. 4(A), j–V characteristics are shown for solar cells made from reference and implanted absorbers with a CdS buffer layer. The reference absorber yields an efficiency of about 14% and it shows negligible changes upon annealing. The implanted absorber shows a strong degradation in V_{oc} as well as in j_{sc} when compared to the reference which can partly be recovered by the annealing step. In order to separate the influences of implantation defects (presumably deep defect levels) and Cd doping (shallow levels), reference implantations were performed with ^{132}Xe ions. No differences between Cd and Xe implantation are detectable in the j–V measurements (not shown). This suggests the observed effects to be mainly due to the implantation defects.

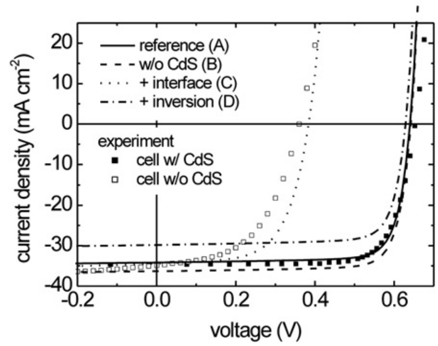

Fig. 2. j–V characteristics simulated with AMPS-1D for the different layer structures (A)–(D) shown in Fig. 1 (lines). As a comparison, experimental data are shown for the cases (A) (reference, full squares) and (C) (cell without CdS after annealing, open squares).

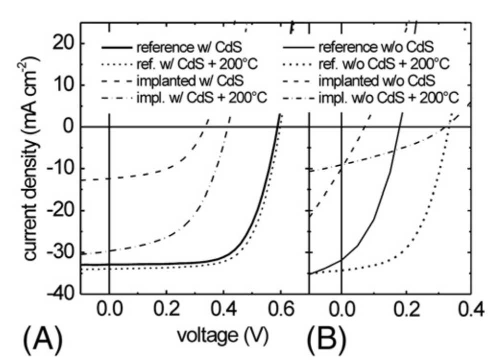

Fig. 4. j–V characteristics of a typical reference sample and of a sample fabricated from Cd-implanted absorbers before and after annealing with (A) and without CdS buffer layer (B).